



Comparative anodic oxidation on boron-doped diamond electrode of two different dyes: separately and mixed

Nour El Houda Abdessamad*, Hanene Akrouf, Latifa Bousselmi

Waste Water Treatment Laboratory, Water Research and Technologies Center (CERTE), Echopark Borj Cedria

Touristic Road of Soliman, BP 273, Soliman 8020, Tunisia

Tel. +216 79 325 044; Fax: +216 79 325 802; email: nour_houda1@yahoo.fr

Received 11 December 2011; Accepted 4 June 2013

ABSTRACT

Two models of azoic and anthraquinone dyes, Acid Orange 8 (AO8) and Alizarin Blue Black B, were chosen to study their electrochemical oxidation on boron-doped diamond electrode separately and in mixture on different proportion. The influence of the initial pH (2 and 8), current density (20, 40, and 80 mA cm⁻²) and their mixture were investigated on discoloration and oxidation kinetics. The results obtained show that the structure of the dyes has an effect on the performance and efficiency of the electrochemical process. Alkaline pH increases anthraquinone dye oxidation rate, while the AO8 azo dye shows a maximum degradation in acidic medium. Moreover, an increase in the current density enhances the rate of degradation of two dyes solution. Study of dyes mixture attests the dependence of the color removal on the nature of predominant dye. Results also show the presence of two kinetic steps, with the first one, which lasts for 30 min, being faster than the second one.

Keywords: BDD electrode; Azoic; Anthraquinone; Mixture; Discoloration; Oxidation

1. Introduction

Industrial effluents contain many types of dyes that are characterized by a strong color, highly fluctuating pH, high chemical oxygen demand (COD), high biological oxygen demand (BOD), and severe biotoxicity [1–3]. In fact, of the 450,000 ton of organic dyes annually produced worldwide, more than 11% is lost in effluents during manufacture and application processes [4]. The most extensively used dyes in textile industry are azo and anthraquinone. Azo dyes account for some 60–70% of the 10,000 commercial

dyes currently in use [5]. Their chromophoric system consists of azo groups (–N=N–) in association with aromatic systems and auxochromes (–OH, –SO₃, etc.) [6]. Anthraquinone dyes belong to the group of most resistant dyes, so they are often used in products that must satisfy strict requirements concerning resistance to solar radiation and ambient conditions. This useful feature of these dyes becomes a problem for their degradation [7].

The conventional treatment processes for the removal of dyes from most effluents before release into the natural system is necessary, but it is very difficult due to their synthetic origin, the high

*Corresponding author.

stability, resistance, and large degree of aromatic rings [8–10]. Electrochemical process is very efficient, as sources of production of reactive species (hydroxyl radicals OH^\bullet), able to degrade highly resistant pollutant molecules and does not require additional chemicals or catalysts [11,12]. One of the most promising processes is certainly the anodic oxidation process [13,14]. Recently, there exists an increasing interest in the use of this technique to decontaminate dyestuff solutions. The effectiveness of this method has been well proven for some persistent dyes including azoic and anthraquinone by using different types of anodes like Pt, RuO_2 , $\text{RuO}_2\text{-TiO}_2$, SnO_2 , and doped and undoped PbO_2 . Better mineralization has been found with the boron-doped diamond (BDD) anodes [15–17].

The great efficiency of BDD electrode to the oxidation of organics pollutant is due in fact to their desirable properties such as a great chemical and electrochemical stability which enhances the average lifetime, high resistance to corrosion, good electrical conductivity, and higher efficiency to electrogenerate hydroxyl radical OH^\bullet [18,19].

BDD electrodes have proven high efficiency in mineralizing of phenol [20], carboxylic acids, 2-naphthol [21], bisphenol [22], benzoic acid [23], and several dyes, such as Orange II [5,15,24], erichrome black T [25], alizarin red S [7,26], amido black [27], and real industrial effluent [28,29].

Real effluents often include more than one component and investigate of the possible interaction between different chromophores will be very useful. However, few authors have focused their research to study the effect of mixture dyes on anodic oxidation [30,31].

Our investigation moved with a twofold aim. First of all, we intended to shade light on the treatment efficiency of aqueous solutions of two dyes separately as anthraquinone and azoic by electrochemical oxidation on BDD electrode. A second purpose was to explore the effect of mixture of these dyes in different proportions in order to study the applicability of this process on industrial field. The effect of pH and applied current density was examined in terms of color removal and organics oxidation.

2. Materials and methods

2.1. Pollutant dye

The oxidation process was investigated using two types of dyes: Acid Orange 8 (AO8, $\text{C}_{17}\text{H}_{13}\text{N}_2\text{NaO}_4\text{S}$; MW = 364.35 g mol^{-1} , purity = 65%) as a model of a mono azoic dye and Alizarin Blue Black B (ABB, $\text{C}_{26}\text{H}_{16}\text{N}_2\text{Na}_2\text{O}_9\text{S}_2$; MW = 610.52 g mol^{-1} , purity = 97%)

as a model of an anthraquinone dye. The initial concentration of the two dyes was 35 mg L^{-1} in all experiments, corresponding to the same COD equal to 60 $\text{mg O}_2 \text{ L}^{-1}$. The mixtures were prepared based on dyes solutions at the following molar ratio: 20% AO8 + 80% ABB, 40% AO8 + 60% ABB, 50% AO8 + 50% ABB, and 60% AO8 + 40% ABB. The chemical structure and absorption spectra of these dyes and their mixtures are reported in Figs. 1(a) and (b).

Absorption spectra in Fig. 1a show that AO8 has two absorption bands (488 and 405 nm) in the visible region related to chromophore-containing azo linkage and two in the UV region (320 and 256 nm) which could be attributed to the $\pi\text{-}\pi^*$ transition of the aromatic ring attached to the -N=N- group in the dye molecule [1,15]. The UV-visible spectra revealed that ABB presents a maximum absorption at 520 nm within the visible range for the presence of carbonyl group and two peaks in the ultraviolet region at 280 and 240 nm for benzenoid and/or quinoid absorption [7]. The UV spectra of the mixture 50% AO8 + 50% ABB (Fig. 1(a)), shows a maximum absorption in the visible region ($\lambda_{\text{max}} = 490 \text{ nm}$) and two absorbance in the UV region at 230 and 310 nm. Results show that the decrease in intensity band is not due to effect of diluted of parental solution but on the effect of the

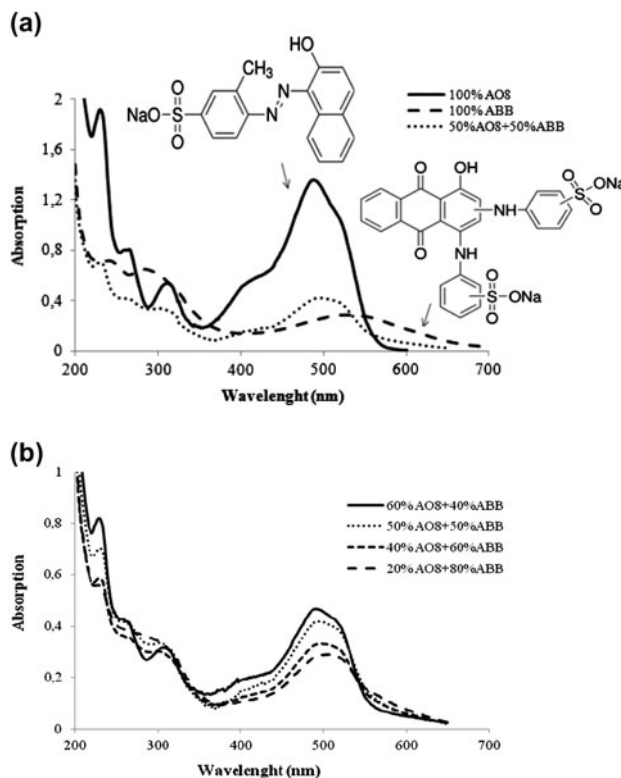


Fig. 1. Absorption spectra of 35 mg L^{-1} (a) AO8 and ABB dyes and (b) their mixture at different proportions.

mixture of two dyes (data not shown). The general aspect of the spectra is the same at different composition of AO8 and ABB dye solutions (Fig. 1(b)) and shows a large absorption band (450–550 nm) with two characteristic peaks of the parent constituents AO8 and ABB dyes (at 488 and 520 nm). However, for the mixture containing 80% ABB, the trend of the spectra tends to be similar to ABB spectra and the UV band appears at 280 nm.

2.2. Chemicals

Distilled water was used throughout for the preparation of aqueous solutions. Na_2SO_4 (99.5%) at 0.1 mol L^{-1} was selected as the support electrolyte. The electrolytic medium was made basic or acidic as required by the addition of aqueous NaOH (0.1 mol L^{-1} [32–35]) or H_2SO_4 (0.1 mol L^{-1}), respectively.

2.3. Electrolysis cell

Electrolysis was conducted in a mini DiaCell (type 500) single-compartment electrolytic cell with parallel plate electrodes manufactured by Adamant Technologies. The anode is a mono-polar Si/BDD, and the cathode is a stainless steel. The active surface area is 12.5 cm^2 , and the electrode gap is 3 mm. The current intensity was provided by a power supply.

Before each experiment, the BDD electrode was subjected to auto cleaning procedure in H_2SO_4 (1 mol L^{-1}) for 30 min. This cleaning is essential for the regeneration of anode because it can remove any possible organic polymer formed at the electrode surface causing reactivity failing [17]. A washing with distilled water is recommended to neutralize the medium. All experiments were performed under galvanostatic mode. The dye solution was stored in a glass tank (1 L) and circulated through the electrolytic cell by means of a peristaltic pump working in recycling mode. The flow rate is fixed at 2.38 L min^{-1} and the temperature at 25°C .

2.4. Analytic procedure

The degradation of the dye solution was monitored by the color and COD removal. The discoloration of the dyes solutions was followed from the drop of their absorbance at the maximum visible wavelength (λ_{max}) of 488 and 520 nm for AO8 and ABB, respectively. The oxidation of the two dyes was then deduced by the (COD) removal of the solution, determined by an open reflux, dichromate titrimetric method as described in standard methods [36].

Color and COD removal ratios were calculated as follows [18]:

$$X \text{ removal (\%)} = \frac{X_0 - X_t}{X_0} \times 100 \quad (1)$$

where X_0 is the initial absorbance values (ABS_0) at λ_{max} and the COD_0 values before treatment, respectively.

X_t is the absorbance values (ABS_t) at λ_{max} and the COD_t values after treatment, respectively.

Electrochemical treatment is undoubtedly an energy-intense process. It is usually assessed in terms of current efficiency (CE) and energy consumption (EC). The CE is defined as the percentage of applied current utilized to reduce COD. It was calculated from COD values using the following relationship [18]:

$$\text{CE} = \frac{[\text{COD}_0 - \text{COD}_t] F V_s}{8 I t} \times 100 \quad (2)$$

where I is the applied current (A), F the Faraday constant, and V_s is the solution volume (L).

The EC is defined as the amount of energy consumed per unit mass of organic load (e.g. dye or COD) removed. The EC per unit COD mass (kWh (g COD)^{-1}) at time t was determined as follows [18]:

$$\text{EC} = \frac{IVt}{[\text{COD}_0 - \text{COD}_t] V_s} \quad (3)$$

where V is the average cell voltage (V) and t is the electrolysis time (h).

Results were expressed by relatively EC to the lowest value as follows:

$$\text{Relative EC \%} = \frac{\text{EC}_t - \text{EC}_1}{\text{EC}_1} \times 100 \quad (4)$$

where EC_1 is the lower value of EC and EC_t is the EC at time t .

3. Results

3.1. Effect of operating conditions on the degradation of AO8 and ABB

To test the effect of solution pH on dyes oxidation, experiments are conducted at pH values 2 and 8. Fig. 2(a) and (b) shows the evolution of the color and COD removal of 35 mg L^{-1} of AO8 and ABB dyes solution at pH 2 and 8 during the anodic oxidation process.

As observed in Fig. 2(a), the complete dye discoloration of AO8 solution is reached approximately at

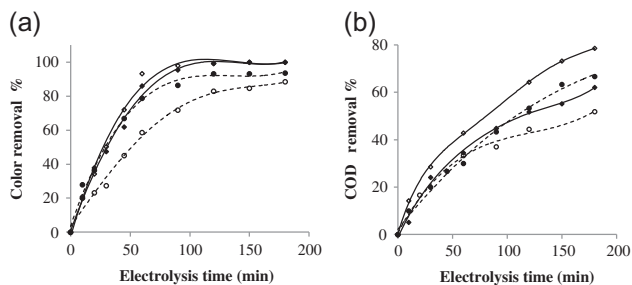


Fig. 2. The variation of the (a) color and (b) COD removal of—AO8 (\diamond , \blacklozenge) and—ABB (\circ , \bullet) with electrolysis time at pH 2 (\diamond or \circ) and at pH 8 (\blacklozenge or \bullet), current density = 40 mA cm^{-2} .

pH 2 and 8, respectively, in 90 and 120 min. At these times, the COD removals achieve only 55 and 51%. The degradation pathway of AO8 dye starts by the cleavage of the most active site by attack of radicals OH. Several papers [37,38] have reported that the fragile group in the azoic dyes is the NH group, which results from an equilibrium between two tautomeric forms, where an H atom is exchanged between O and N as shown in Fig. 3.

Indeed, the abstraction of H atom (carried by an oxygen atom in the azo form and by a nitrogen atom in the hydrazone form) by OH radicals is the main degradation pathway of the azoic dyes. Moreover, the increase in the percentage of color removal with the electrolysis time is not proportional with the increase in COD removal. This behavior can be explained by the fact that the oxidation of the azo group is accompanied by the formation of several aromatic by-products and later their oxidations continue [39].

For ABB solution dye, 88 and 94% of color removal and 52 and 66% of COD reduction at pH 2 and 8, respectively, are attained after 180 min. Only few papers discussed the oxidation mechanism of anthraquinone dye. The cleavage of the aromatic ring in the C=C bond near the C=O group to form colorless intermediates (mainly phthalic acid, small carbonyl species) was proposed as first step [40], these intermediates are completely mineralized to carbon dioxide. The production of acidic intermediate is verified by following pH in solution during anodic

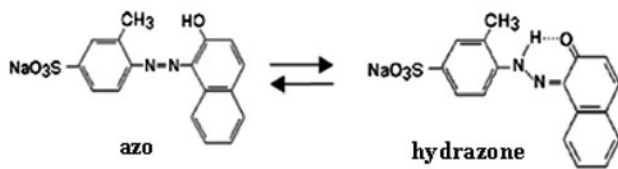


Fig. 3. Equilibrium between the two tautomeric forms in AO8.

oxidation process which remains constant at initial pH = 2, while at initial pH equal to 8, the pH decreases to 5 (Fig. 4).

The ABB color and COD percentages removal are lesser than obtained in the case of AO8. This result reveals that the ABB molecule which includes five benzoic groups and a high degree of aromaticity is a more recalcitrant compound than the AO8.

The kinetic analyses of the above results have good linear correlations when they were fitted with a pseudo-first-order reaction rate equation. Pseudo-first-order rate constants are summarize in Table 1.

According to Fig. 2 and Table 1, the degradation kinetics notably depends upon the basic molecular structure of the dyes and the pH of solution dye.

The degradation of AO8 is favored at acidic conditions ($k_{\text{discoloration}}(\text{pH } 2) = 0.030 \text{ min}^{-1}$ $k_{\text{discoloration}}(\text{pH } 8) = 0.026 \text{ min}^{-1}$). It should be noted that the pH of dye solution strongly affect the production of reactive radicals at the surface of BDD electrode. The generation of radical hydroxyl is favored in acidic medium. Therefore, the degradation rate of AO8 enhances in pH 2. On the other hand, alkaline conditions appear to favor color and COD reduction in the case of ABB dye. This suggests that the basic medium favors the production of structures that are more easily oxidizable by the hydroxyl radical [41]. Moreover, the results obtained by Sun et al. [26] show that the alkaline medium seems to favor the deprotonation of groups adjacent to quinine function (NH and OH). Then, at the beginning of the electrolysis, the cleavage of the bonds responsible for the color occurred so that the molecule of dye loses the conjugated transition absorbing in visible region.

The following of the evolution of pH during the oxidation of the two dyes at pH 2 and 8 confirm these

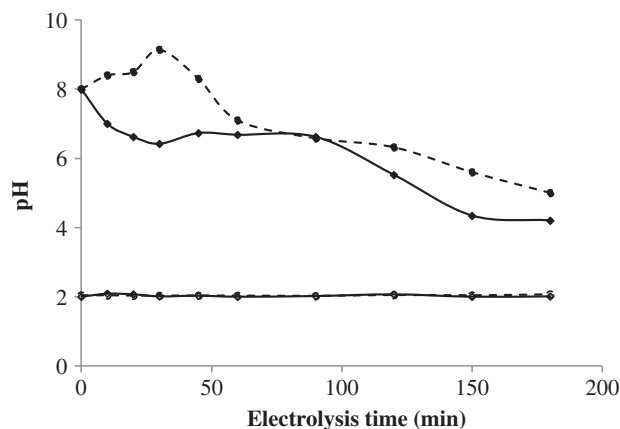


Fig. 4. The variation of the pH of—AO8 (\diamond or \circ) and—ABB (\blacklozenge or \bullet) with electrolysis time at pH 2 (\diamond or \circ) and at pH 8 (\blacklozenge or \bullet), current density = 40 mA cm^{-2} .

Table 1

The pseudo-first-order rate constant (k) values for anodic oxidation of the AO8 and ABB solution dyes at different pH, $[Dye]_0 = 35 \text{ mg L}^{-1}$, 40 mA cm^{-2}

	ABB		AO8	
	pH 2	pH 8	pH 2	pH 8
$k_{\text{discoloration}} 10^{-3} \text{ min}^{-1}$	14.2 ($R^2=0.99$)	23.1 ($R^2=0.98$)	30 ($R^2=0.99$)	26 ($R^2=0.98$)
$k_{\text{global degradation}} 10^{-3} \text{ min}^{-1}$	5.2 ($R^2=0.95$)	6.4 ($R^2=0.98$)	8 ($R^2=0.97$)	4.3 ($R^2=0.98$)

hypotheses. Indeed, Fig. 4 shows that at pH 2, the pH remains constant in the two cases during the electrolysis time; however, at pH 8, the behavior is different. For ABB dye, the pH increase at the first 20 min is justified by the production of alkaline species, and then, it decreases to 5 due to the presence of acidic species. Concerning AO8 dye, the pH decreases slowly from 8 to 4 indicating the formation of acidic by-products.

As seen also in Table 1, the degradation of AO8 is favored at pH 2. The CE and the relative EC required to mineralize 35 mg L^{-1} of AO8 and ABB dyes solution ($V = 1 \text{ L}$) at pH 2 for AO8 and 8 for ABB have been investigated (Fig. 5).

At the beginning of electrolysis, a high current efficiency is observed for the two dyes (Fig. 5). This is related to the quick decomposition of AO8 and ABB on aromatic derivatives [42] which are more easily oxidizable than the ring opening products reached at the end of electrolysis and requiring more energy.

The percentage of current efficiency of AO8 after discoloration of solution (90 min), decrease three times compared with the initial value of CE due to the production of colorless and recalcitrant intermediates. The relative EC is enhanced 133% of lower initial EC. This behavior, characteristic of electrochemical treatment, is also explained in terms of mass transfer limitations [43].

As seen also in Fig. 5, the oxidation of ABB dye presented lower current efficiencies and required more energy compared with the oxidation of AO8.

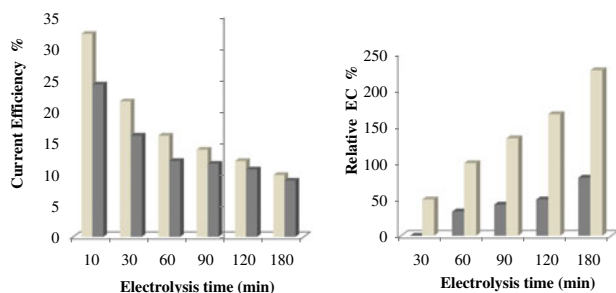


Fig. 5. Evolution of CE and EC of 35 mg L^{-1} of AO8 (clear) and ABB (dark) dyes with time at the optimum pH and under 40 mA cm^{-2} .

Nevertheless, it is clearly that the difference between the CE values of AO8 and ABB at the first times of electrolysis, and particularly before the total discoloration time, is significant. Indeed, the oxidation of ABB required more than twice the energy required for the oxidation of AO8 due to the recalcitrant nature of ABB. At the end of electrolysis, the trend of CE of two dyes is expected to be similar. In fact, several studies on several dyes molecules mineralization prove the formation of carboxylic acids at this final stage. However, in this stage, the EC gap between the two studied dyes is still important due to the quantity of residual COD of ABB which still higher (35%) [26]. This result confirms again that the azoic bond is more easily degraded by hydroxyl radicals than the chromophore anthraquinone compound ABB dye with high molecular weight and higher degree of conjugation formed a recalcitrant compound compared with the azoic dye.

The effect of current density value (20, 40, and 80 mA cm^{-2}) in the oxidation of the two dyes at pH which proved to be more efficient for the oxidation was investigated in order to add more insights (Fig. 6).

As seen in Fig. 6, for AO8 solution, the increase in current density from 20 to 40 mA cm^{-2} decreases the time necessary for total discoloration, while a negligible effect is observed when current density increases from 40 to 80 mA cm^{-2} . Moreover, the COD removal increases from 56% at 20 mA cm^{-2} to 90% at 80 mA cm^{-2} .

For ABB solution, the behavior is different. The increase in current intensity increases always the color removal. At 120 min of electrolysis, 86, 93, and 99% of discoloration and 38, 53, and 65% of COD removal can be observed for 20, 40, and 80 mA cm^{-2} , respectively. This trend can be accounted for the increased production of hydroxyl radicals OH^\bullet and other oxidants such as ozone, peroxodisulfate ion $\text{S}_2\text{O}_8^{2-}$ and hydroxide peroxide H_2O_2 at the surface of BDD anode and/or in the solution [18].

The generation of these oxidants species can be greatly improved with increasing current density,

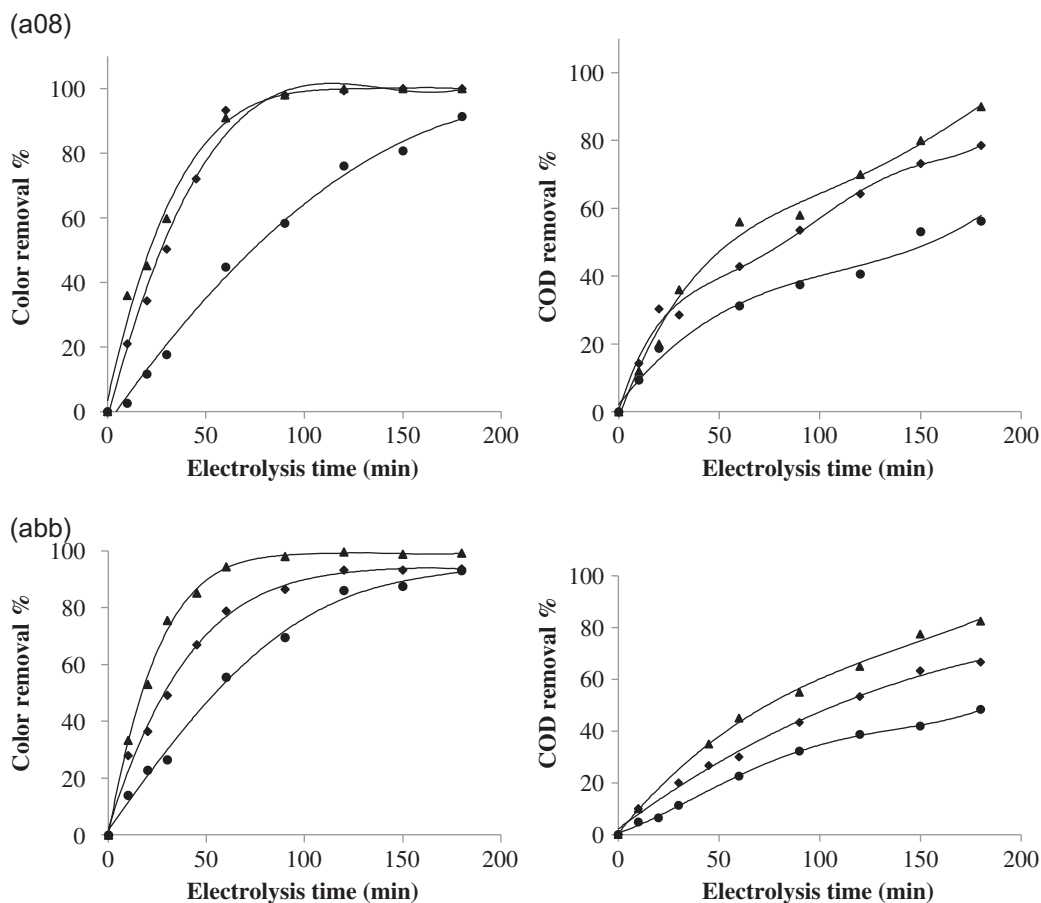


Fig. 6. The variation of the color (a) and COD (b) removal of AO8 and ABB dyes with electrolysis time at different current density: (●) 20, (◆) 40 and (▲) 80 mA cm⁻².

which enhances the destruction of the dye and hence, enhances the discoloration and oxidation rate of the solution.

The constants rates thus obtained for three different current densities are summarized in Table 2. The percentage of discoloration, the CE discoloration of AO8 dye solution at pH 2 (90 min), used as reference, are also shown in Table 2.

As seen in Table 2, a progressive increase in color and COD rate removal is obtained when current density rises in all cases studied. In fact, an increase in the current density enhances the degradation rate of ABB and AO8, this behavior is characteristic of mass transfer control [24]. A decrease in the current efficiency CE is noted also when applied current density increases. This is due to the fact that part of

Table 2

The pseudo-first-order rate constant (k) values for discoloration and oxidation of the AO8 and ABB solution dyes, the percentage of color, COD removal, CE at 90 min at different current density, [Dye]₀ = 35 mg L⁻¹

Current density mA cm ⁻²	20		40		80	
	ABB	AO8	ABB	AO8	ABB	AO8
k _{discoloration} 10 ⁻³ min ⁻¹	14.8 (R ² = 0.98)	10 (R ² = 0.98)	23.1 (R ² = 0.98)	30 (R ² = 0.99)	45.2 (R ² = 0.99)	39 (R ² = 0.98)
k _{global degradation} 10 ⁻³ min ⁻¹	4.1 (R ² = 0.91)	4 (R ² = 0.94)	6.4 (R ² = 0.98)	8 (R ² = 0.97)	9.1 (R ² = 0.99)	10 (R ² = 0.98)
Color removal % at 90 min	69	58	86	98	98	100
COD removal % at 90 min	32	37.5	43	54	55	58
CE % at 90 min	18	21	12	13	5	6

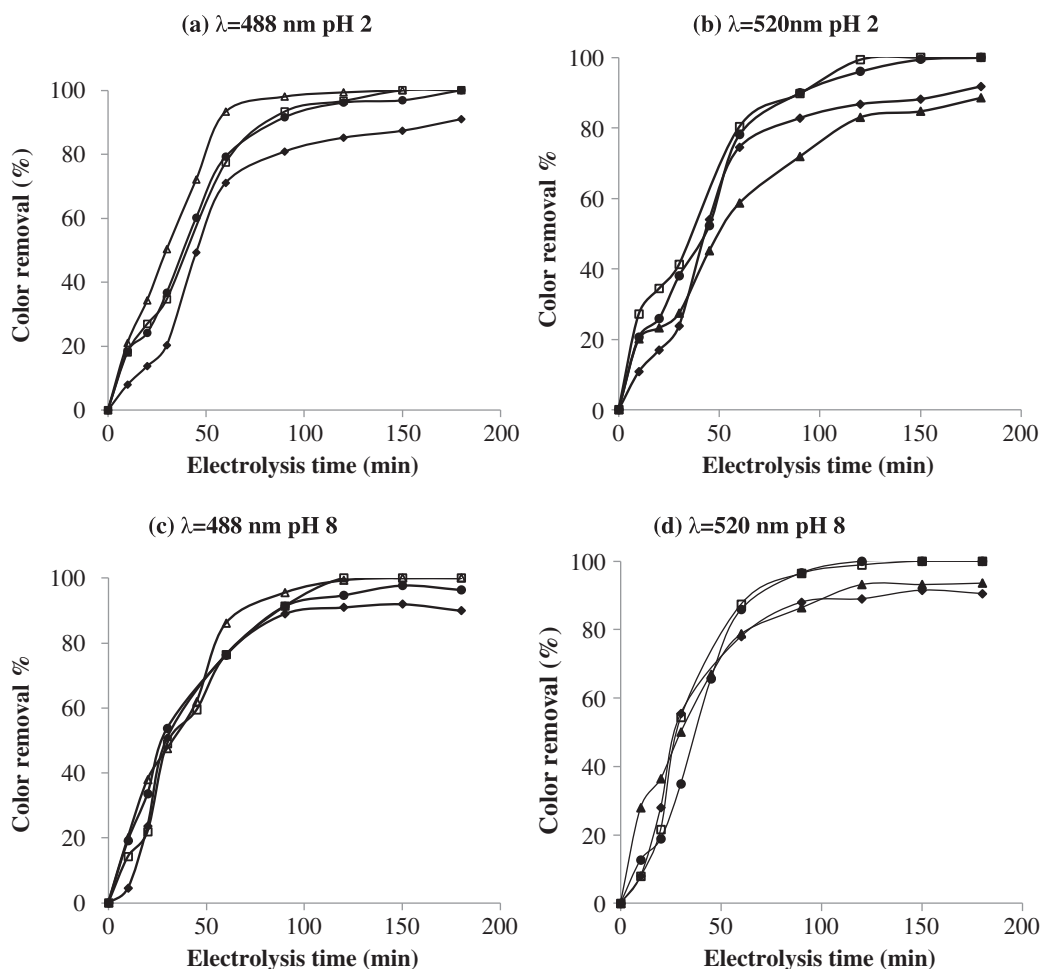


Fig. 7. The variation of the color removal of dyes mixture with electrolysis time (□) 60% AO8 + 40% ABB, (●) 50% AO8 + 50% ABB, (◆) 20% AO8 + 80% ABB, (Δ) 100% AO8 and (▲) 100% ABB at pH 2 and 8, current density = 40 mA cm^{-2} .

the electrogenerated radicals are wasted to side reactions such as O_2 evolution [44] but also in the case of ABB to the generation of more recalcitrant compounds as concluded by the precedent results and observed in previous study for oxidation of Alizarin Red S [15,26].

3.2. Effect of mixture of dyes

Real textile effluents often contain multiple dyes and the study of the possible interactions between different chromophoric groups during the treatment may be useful. In this paper, the effect of mixture in different proportions of the azoic and anthraquinone dyes already studied was investigated at pH 2 and 8. The color removal of the mixture of different composition of AO8 and ABB dye solutions was determined at the two characteristic peaks of each dye, at $\lambda=488$ nm (wavelength characteristic of AO8 dye) and 520 nm (wavelength characteristic of ABB dye) [45]. Investigation was made at the two pHs 2 and 8 (Fig. 7).

As seen in Fig. 7, dependence of the color removal on the nature of predominant dye in mixture solution is observed. Indeed, almost the same behavior is noted if we follow the removal of AO8 dye at 488 nm in mixture solution especially for pH 2. At this pH, the time of discoloration decreases when the proportion of AO8 dye increases. In all proportion of dyes mixture, total discoloration is reached after 180 min of treatment except that containing 20% AO8 and 80% ABB which achieve only 90% of color removal. ABB is acting as inhibitor to AO8 discoloration.

It was noted that the increase in AO8 proportion increases the removal of its color at corresponding wavelength maximum. This can be explained by the predominance of the AO8 dye and its by-products compared with ABB. The predominant species influences the discoloration rate of the solution. Thus, the presence of AO8, which is more easily oxidized, favors the degradation of the dye solution. This behavior is less pronounced at pH 8 and especially

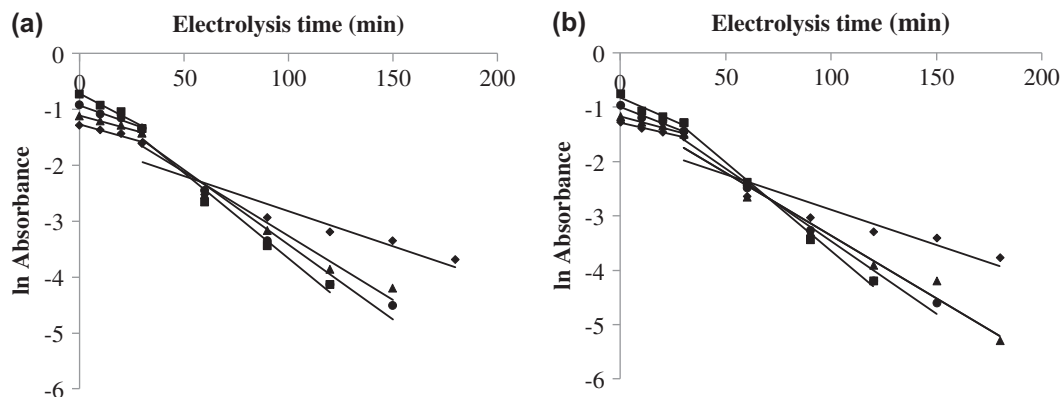


Fig. 8. Absorbance variation with electrolysis time t (min) at (a) 488 and (b) 520 nm peaks during the electrolysis time: (◆) 20% (▲) 40% (●) 50% (■) 60%, pH 2.

when we follow the color removal at 520 nm, wavelength characteristic of ABB dye. This can be explained by the fact that at this wavelength, the AO8 dye shows also an important intensity band which can interfere with the results and make the color removal calculated not corresponding at removal of ABB alone.

At the beginning of the electrolysis, it should be noted that the trend of the evolution of color removal is approximately similar. This behavior reveals the production of competitive reactions between species present in solution including; oxidative species electrogenerated at the surface at BDD electrodes, AO8 and ABB dyes, as well as their by-products. In fact, the OH^\bullet produced attack generally the most active site. Results obtained show that this site is probably the azoic bond since that the AO8 dye presents a synergic effect.

In the case of mixture containing the same proportion of AO8 and ABB dyes, the rate showed at 488 nm is higher than the rate obtained at 520 nm.

The kinetic analysis is investigated at pH 2 (Fig. 8). Two distinct disappearance rates are shown at each wavelength (488 nm for AO8 and 520 nm for ABB) and might be connected with different mechanisms.

Two successive first-order kinetic steps are involved in the overall degradation process, and the first one lasts less than 30 min.

The constant kinetic rates of each step measured at 488 and 520 nm for all studied mixtures at pH 2, as well as the rate of oxidation are illustrated in Table 3.

Results show the presence of two kinetic steps, with the first one, which lasts for 30 min, being faster than the second one. The increase in the rate of discoloration at 488 and 520 nm is observed with the increase in AO8 dye but it is more pronounced at 520 nm. This fact seems to be due to the lower absorption of ABB at this wavelength compared with AO8. Therefore, the decrease in its intensity bands is faster.

It should be noted also that the rate of the oxidation is not affected significantly by the variations of the proportion of dye in the mixture solution.

Table 3

The pseudo-first-order rate constant (k) values for anodic oxidation of the different mixture of AO8 and ABB solution dyes at pH 2, $[\text{AO8} + \text{ABB}]_0 = 35 \text{ mg L}^{-1}$

AO8/ABB (%)	$k \cdot 10^{-3} \text{ (min}^{-1}\text{)}$				k_{COD}	
	0–30 min		30 min– $t_{\text{discoloration}}$		pH 2	pH 8
	$\lambda = 488 \text{ nm}$	$\lambda = 520 \text{ nm}$	$\lambda = 488 \text{ nm}$	$\lambda = 520 \text{ nm}$		
20/80	9.3 ($R^2 = 0.96$)	8.8 ($R^2 = 0.99$)	9.1 ($R^2 = 0.98$)	8.8 ($R^2 = 0.97$)	6.2 ($R^2 = 0.99$)	4.1 ($R^2 = 0.99$)
40/60	10 ($R^2 = 0.98$)	10.4 ($R^2 = 0.97$)	19.1 ($R^2 = 0.98$)	20.6 ($R^2 = 0.95$)	5.9 ($R^2 = 0.99$)	4.1 ($R^2 = 0.99$)
50/50	13.3 ($R^2 = 0.98$)	15 ($R^2 = 0.96$)	23.2 ($R^2 = 0.97$)	24.3 ($R^2 = 0.99$)	6.1 ($R^2 = 0.99$)	5 ($R^2 = 0.99$)
60/40	19.7 ($R^2 = 0.98$)	17 ($R^2 = 0.92$)	24.6 ($R^2 = 0.99$)	30.2 ($R^2 = 0.99$)	6.3 ($R^2 = 0.99$)	4.9 ($R^2 = 0.99$)

Whereas the initial COD; composed of ABB or AO8 dye; is maintained constant with the different proportion, the same degradation of COD is obtained. This result is consistent with a non-selective oxidation of organic compounds (dyes) on BDD electrode which is mainly due to the reactivity of OH[•].

4. Conclusion

The present study demonstrates that the structure of the dyes affects the discoloration and the oxidation of dye solution treated by anodic oxidation on BDD electrodes. The results obtained show that the degradation of AO8 is clearly favored at acidic conditions, whereas the alkaline conditions, improve the ABB oxidation. So, the complete dye discoloration of AO8 solution is reached approximately in 90 and 120 min at pH 2 and 8, respectively, and the COD removal achieves about 62 and 78% after 180 min of electrolysis. For ABB dye solution, 88 and 94% of color removal and 52 and 66% of COD reduction at pH 2 and 8, respectively, are attained after 180 min. Moreover, an increase in the current density leads to an increase in the rate of degradation of ABB and AO8. The current density equal to 40 mA cm⁻² is sufficient to achieve a completely discoloration of AO8 dye solution at pH 2 with 80% of COD removal. Study of dye mixture reveals the dependence of the color removal on the nature of predominant dye. Results show also the presence of two kinetic steps with the first one which being 60 times faster than the second one.

Acknowledgments

This research was done with the support of International Foundation for Science (IFS), Sweden, by a research following ship to CP: Hanene Akrouit – Baccour.

Authors acknowledge also “Capacity Building for Direct Water Reuse in the Mediterranean Area (CB-WR-MED)” project financed by Seventh Framework Program (FP7) and contract objective project financed by Ministry of Higher Education and Scientific Research in Tunisia.

References

- [1] M.F. Elahmadi, N. Bensalah, A. Gadri, Treatment of aqueous wastes contaminated with Congo Red dye by electrochemical oxidation and ozonation processes, *J. Hazard. Mater.* 168 (2009) 1163–1169.
- [2] B. Kayan, B. G. zmen, M. Demirel, A.M. Gizir, Degradation of acid red 97 dye in aqueous medium using wet oxidation and electro-Fenton techniques, *J. Hazard. Mater.* 177 (2010) 95–102.
- [3] A. Wang, J. Qu, H. Liu, J. Ge, Degradation of azo dye acid red 14 in aqueous solution by electrokinetic and electrooxidation process, *Chemosphere* 55 (2004) 1189–1196.
- [4] S. Parsons, *Advanced Oxidation Processes for Water and Wastewater Treatment*. IWA Publishing, London, 2004.
- [5] A. Fernandes, A. Morao, M. Magrinho, A. Lopes, I. Gonçalves, Electrochemical degradation of C.I. acid orange 7, *Dyes Pigm.* 61 (2004) 287–296.
- [6] T.M. Elmorsi, Y.M. Riyad, Z.H. Mohamed, H.M.H. Abd El Bary, Decolorization of mordant red 73 azo dye in water using H₂O₂/UV and photo-Fenton treatment, *J. Hazard. Mater.* 174 (2010) 352–358.
- [7] A.M. Faouzi, B. Nasr, G. Abdellatif, Electrochemical degradation of anthraquinone dye alizarin red S by anodic oxidation on boron-doped diamond, *Dyes Pigm.* 73 (2007) 86–89.
- [8] M. Panizza, G. Cerisola, Removal of colour and COD from wastewater containing acid blue 22 by electrochemical oxidation, *J. Hazard. Mater.* 153 (2008) 83–88.
- [9] C. Flox, S. Ammar, C. Arias, E. Brillas, A.V. Vargas-Zavala, R. Abdelhedi, Electro-Fenton and photoelectro-Fenton degradation of indigo carmine in acidic aqueous medium, *Appl. Catal. B* 67 (2006) 93–104.
- [10] I. del Río, J. Fernandez, J. Molina, J. Bonastre, F. Cases, Electrochemical treatment of a synthetic wastewater containing a sulphonated azo dye. Determination of naphthalenesulphonic compounds produced as main by-products, *Desalination* 273 (2011) 428–435.
- [11] X. Chen, G. Chen, P.L. Yue, Anodic oxidation of dyes at novel Ti/B-diamond electrodes, *Chem. Eng. Sci.* 58 (2003) 995–1001.
- [12] L. Fan, Y. Zhou, W. Yang, G. Chen, F. Yang, Electrochemical degradation of Amaranth aqueous solution on ACF, *J. Hazard. Mater. B* 137 (2006) 1182–1188.
- [13] K. Swaminathan Sarayu, S. Sandhya, Assessment of degradation of eight commercial reactive azo dyes individually and in mixture in aqueous solution by ozonation, *Dyes Pigm.* 75 (2007) 362–368.
- [14] S. Hammami, M.A. Oturan, N. Oturan, N. Bellakhal, M. Dac-hraoui, Comparative mineralization of textile dye indigo by photo-Fenton process and anodic oxidation using boron-doped diamond anode, *Desalin. Water Treat.* 45 (2012) 297–304.
- [15] S. Hammami, N. Bellakhal, N. Oturan, M.A. Oturan, M. Dac-hraoui, Degradation of acid orange 7 by electrochemically generated OH[•] radicals in acidic aqueous medium using a boron-doped diamond or platinum anode: A mechanistic study, *Chemosphere* 73 (2008) 678–684.
- [16] M. Hamza, R. Abdelhedi, E. Brillas, I. Sires, Comparative electrochemical degradation of the triphenylmethane dye methyl violet with boron-doped diamond and Pt anodes, *J. Electroanal. Chem.* 627 (2009) 41–50.
- [17] N. El Houda Abdessamad, H. Akrouit, L. Bousselmi, Evaluation and optimization of textile synthetic effluent discoloration using anodic oxidation on BDD electrode: Application of the experimental design methodology, *Desalin. Wat. Treat.* 51(16–18) (2013) 3428–3437.
- [18] C.A. Martinez-Huitle, E. Brillas, Decontamination of wastewaters containing synthetic organic dyes by electrochemical methods: A general review, *Appl. Catal. B* 87 (2009) 105–145.
- [19] A. Kraft, M. Stadelmann, M. Blaschke, Anodic oxidation with doped diamond electrodes: A new advanced oxidation process, *J. Hazard. Mater. B* 103 (2003) 247–261.
- [20] J. Iniesta, P.A. Michaud, M. Panizza, G. Cerisola, A. Aldaz, C. Comninellis, Electrochemical oxidation of phenol at boron-doped diamond electrode, *Electrochim. Acta* 46 (2001) 3573–3578.
- [21] M. Panizza, P.A. Michaud, G. Cerisola, Ch. Comninellis, Anodic oxidation of 2-naphthol at boron-doped diamond electrodes, *J. Electroanal. Chem.* 507 (2001) 206–214.
- [22] M. Muruganathan, S. Yoshihara, T. Rakuma, T. Shirakashi, Mineralization of bisphenol A (BPA) by anodic oxidation with boron-doped diamond (BDD) electrode, *J. Hazard. Mater.* 154 (2008) 213–220.

- [23] F. Montilla, P.A. Michaud, E. Morallón, J.L. Vázquez, Ch. Comninellis, Electrochemical oxidation of benzoic acid at boron-doped diamond electrodes, *Electrochim. Acta* 47 (2002) 3509–3513.
- [24] X. Chen, G. Chen, Anodic oxidation of orange II on Ti/BDD electrode: Variable effects, *Sep. Purif. Technol.* 48 (2006) 45–49.
- [25] A. Bedoui, M.F. Ahmadi, N. Bensalah, A. Gadri, Comparative study of eriochrome black T treatment by BDD-anodic oxidation and Fenton process, *J. Chem. Eng.* 146 (2009) 98–104.
- [26] J. Sun, H. Lu, L. Du, H. Lin, H. Li, Anodic oxidation of anthraquinone dye alizarin red S at Ti/BDD electrodes, *Appl. Surf. Sci.* 257 (2011) 6667–6671.
- [27] H. Akrouf, L. Bouselmi, Chloride ions as an agent promoting the oxidation of synthetic dyestuff on BDD electrode, *Desalin. Wat. Treat.* 46 (2012) 171–181.
- [28] E. Tsantaki, T. Velegriki, A. Katsaounis, D. Mantzavinos, Anodic oxidation of textile dye house effluents on boron-doped diamond electrode, *J. Hazard. Mater.* 207–208 (2011) 91–96.
- [29] E. Chatzisyneon, N.P. Xekoukoulotakis, A. Coz, N. Kalogerakis, D. Mantzavinos, Electrochemical treatment of textile dyes and dyehouse effluents, *J. Hazard. Mater. B.* 137 (2006) 998–1007.
- [30] A.R. Khataee, M.B. Kasiri, Photocatalytic degradation of organic dyes in the presence of nanostructured titanium dioxide: Influence of the chemical structure of dyes, *J. Mol. Catal. A: Chem.* 328 (2010) 8–26.
- [31] M. Fathinia, A.R. Khataee, M. Zarei, S. Aber, Comparative photocatalytic degradation of two dyes on immobilized TiO₂ nanoparticles: Effect of dye molecular structure and response surface approach, *J. Mol. Catal. A: Chem.* 333 (2010) 73–84.
- [32] M. Muruganathan, S. Yoshihara, T. Rakuma, N. Uehara, T. Shirakashi, Electrochemical degradation of 17 β estradiol (E2) at boron-doped diamond (Si/BDD) thin film electrode, *Electrochim. Acta* 52 (2007) 3242–3249.
- [33] L.S. Andrade, T.T. Tasso, D.L. da Silva, R.C. Rocha-Filho, N. Bocchi, S.R. Biaggio, On the performances of lead dioxide and boron-doped diamond electrodes in the anodic oxidation of simulated wastewater containing the reactive orange 16 dye, *Electrochim. Acta* 54 (2009) 2024–2030.
- [34] A.I. del Río, J. Molina, J. Bonastre, F. Cases, Influence of electrochemical reduction and oxidation processes on the decolourisation and degradation of C.I. reactive orange 4 solutions, *Chemosphere* 75 (2009) 1329–1337.
- [35] X. Zhao, Y. Hou, H. Liu, Z. Qiang, J. Qu, Electro-oxidation of diclofenac at boron doped diamond: Kinetics and mechanism, *Electrochim. Acta* 54 (2009) 4172–4179.
- [36] APHA, AWWA, WPCF, Standard Methods for the Examination of Water and Wastewater, 20th ed., APHA, AWWA, WPCF, Washington, DC, 1998.
- [37] A.R. Khataee, M.N. Pons, O. Zahraa, Photocatalytic degradation of three azo dyes using immobilized TiO₂ nanoparticles on glass plates activated by UV light irradiation: Influence of dye molecular structure, *J. Hazard. Mater.* 168 (2009) 451–457.
- [38] A.R. Khataee, M.N. Pons, O. Zahraa, Photocatalytic decolorisation and mineralization of orange dyes on immobilized titanium dioxide nanoparticles, *Water Sci. Technol.* 62 (2010) 1112–1120.
- [39] C. Saez, M. Panizza, M.A. Rodrigo, G. Cerisola, Electrochemical incineration of dyes using a boron-doped diamond anode, *J. Chem. Technol. Biotechnol.* 82 (2007) 575–581.
- [40] M. Panizza, G. Cerisola, Electro-Fenton degradation of synthetic dyes, *Water Res.* 43 (2009) 339–344.
- [41] M. Panizza, M.A. Oturan, Degradation of alizarin red by electro-Fenton process using a graphite-felt cathode, *Electrochim. Acta* 56 (2011) 7084–7087.
- [42] Ch. Comninellis, E. Plattner, Electrochemical wastewater treatment, *Chimia* 42 (1988) 250–252.
- [43] B. Nasr, T. Hsen, G. Abdellatif, Electrochemical treatment of aqueous wastes containing pyrogallol by BDD-anodic oxidation, *J. Environ. Manage.* 90 (2009) 523–530.
- [44] I. Sires, P.L. Cabot, F. Centellas, J.A. Garrido, R.M. Rodríguez, C. Arias, E. Brillas, Electrochemical degradation of clofibrac acid in water by anodic oxidation: Comparative study with platinum and boron-doped diamond electrodes, *Electrochim. Acta* 52 (2006) 75–85.
- [45] F. Abdelmalek, S. Gharbi, B. Benstaali, A. Addou, J.L. Brisset, Plasmachemical degradation of azo dyes by humid air plasma: yellow supranol 4 GL, scarlet red nylosan F3 GL and industrial waste, *Water Res.* 38 (2004) 2339–2347.